J. Earth Syst. Sci. (2020)129 27
https://doi.org/10.1007/s12040-019-1275-6

Seismic imaging of subsurface geological structures by Kirchhoff's migration based on extended Born approximation

Alok Kumar Routa* and P R Mohanty

Department of Applied Geophysics, Indian Institute of Technology (ISM), Dhanbad, Dhanbad, India.
**Corresponding author. e-mail: alokkumar.routa93@gmail.com*

MS received 21 November 2018; revised 4 April 2019; accepted 29 July 2019

Complex seismic signatures are generated because of the multifaceted nature of the subsurface. These features make the interpretation very complex. To understand the seismic behaviour, different numerical tools are available. In this present study, an attempt has been made to demonstrate both the modelling and imaging aspects of these complex subsurface features commonly encountered in petroleum exploration. The present work is an extended form of the Born approximation by using Green's function based asymptotic ray theory. Subsequently, Kirchhoff's depth migration has been applied to generate seismic shot gathers over structural as well as stratigraphic traps. From this analysis, it is observed that the technique is able to efficiently migrate both the structural and stratigraphic traps. The proposed technique also intends to handle strong velocity variation and amplitude restoration. However, some noise in terms of over-critical reflection has been observed in the depth migrated section corresponding to pinch-out and unconformity respectively.

Keywords. Asymptotic ray tracing method; Born approximation; forward modelling; Kirchhoff's migration.

1. Introduction

Seismic modelling is one of the essential tools broadly utilized as a part of seismic processing and interpretation. Two main stages of seismic modelling are geological model building and numerical computation of seismic response of the model. In this way, the model building approaches become equally important as seismic forward realization methods (Alaei 2012). Numerical modelling of seismic information is characterized as the utilization of a geological model of the Earth to reproduce seismic field tests. The most widely accepted utilization of the forward modelling is to determine the seismic response of some expected features of the subsurface geology. Besides these, forward modelling also used to substantiate the structural as well as the stratigraphic understanding. Models are really considered to be the representation of factual objects might be of 1D, 2D or 3D. Different types of seismic modelling techniques are performed among which, Ray tracing methods are very frequently used in seismic modelling and imaging (Carcione *et al.* 2002). This Ray tracing theory used energy in the form of rays: which goes along least time paths in the desired model. This principally follows the concept of Snell's law. As per this phenomenon when velocity changes, rays bend and partially reflected when it meets velocity or density drop. There are several approximate

Published online: 20 December 2019

methods available based on Asymptotic Ray Theory (ART); these include geometrical ray theory, Maslov ray theory, the Gaussian beam method, etc., which model geometrical properties of wave fronts and signals scattered by discontinuities of the model (Chapman and Coates 1994). In any case, all the above methods cannot model the partial reflections produced by the continuous gradient. Except this, in ray tracing, minimum travel time path for point diffraction appear at a point displaced to the side with higher velocity rather than the surface directly above to it. Applying the diffraction stack process in a practical situation means that some approximation is required (Kirk 1981). To overcome this problem in this present study, extended Born approximation tool is used for modelling purposes. For the study of exploration seismology, the Born approximation is highly appealing due to its simplicity and relative efficiency (Parisi *et al.* 2015). This ray Born modelling can also generate synthetic data with predominance conditions. This technique was discussed by Parisi *et al.* (2015) about the phase modelling of the subsurface, Chapman and Coates (1994) about the scattering in anisotropic media, Jakobsen (2012) about forward modelling in acoustic approximation. In addition, Capdeville *et al.* (2002), Tromp *et al.* (2005), Romanowicz *et al.* (2008), Panning *et al.* (2009), Peter *et al.* (2009) and Dalton *et al.* (2013) had investigated how good the Born approximation is to compute synthetic seismograms. They all clarified the algorithm of this Born approximation, connected to some basic models like a small cavity, a single grid point or simple mantle and crust model. But none of them discussed whether this technique is either adequate towards the complexity of the subsurface or not. Wang *et al.* (2004) mentioned a disadvantage of this method that, it could not handle strong velocity variation in the medium.

Later in the year 2016, Huang *et al.* discussed a similar type of approximation using Gaussian beam summation based on classical geometric ray theory applied to only modelling purpose.

To overcome all the demerits mentioned above, the study is divided into two parts: at first, we extend the Born approximation by using the Green's function based on asymptotic ray theory for forward modelling and perform Kirchhoff's migration using that extended Born approximation. In addition, strong velocity variation was considered in the present study, which was not earlier shown in the paper of Wang *et al.* (2004). In seismic migration, the reflectivity of geological boundaries is estimated, resulting in a structural image of subsurface (Clearbout 1985; Berkhout 2012). At first, we review the Born scattering theory. Secondly, construct the Born approximation modelling for Kirchhoff's migration. For the numerical synthetic test, we simulate different types of structural as well as stratigraphic velocity models and resize one exiting synthetic model.

2. Mathematical background

Here, the basic mathematical formulation for ray tracing is illustrated. There exists two major approaches to the derivation of the ray equation. The former is based on the classical approach dealing with Heuristic geometric principle usually called Geometric Ray Theory (GRT). The second one derives the ray equation from the wave equation by means of asymptotic analysis referred as Asymptotic Ray Theory (ART); which is accounted for the present analysis. The analysis starts by considering a velocity model which is inhomogeneous in nature. The inhomogeneous velocity model is nothing but the sum of the background velocity model, which deviate slowly and a scatter one that deviates rapidly.

Mathematically;

$$v(x) = v_0(x) + \delta v_1(x) = v_0[1 + \epsilon(x)] \qquad (1)$$

where $\epsilon > 0$ is a dimensionless parameter. Now consider the wave equation of velocity model in frequency domain (Chapman 2004):

$$s(x,\omega) = \omega^2 v^{-2}(x) u(x,\omega) + \Delta u(x,\omega) \qquad (2)$$

where $s(x,\omega)$ is the source function, $u(x,\omega)$ is the x dependent wave function and Δ is the Laplace operator. Here for a point source y, the Green's function g_0 performed as the background function which may be written as:

$$\delta(x-y) = \omega^2 v_0^{-2}(x) g_0(x,y,\omega) + \Delta g_0(x,y,\omega). \quad (3)$$

According to this for $v_1 \equiv 0$, the solution of equation (2) is the background waveu_0 is mathematically:

$$u_0(x,\omega) = \int g_0(x,y,\omega) s(y,\omega)\, dy. \qquad (4)$$

This is for the total source area. The common solution obtained for scattering is written below.

$$u = \sum_{k=0}^{\infty} u_k \epsilon^k = u_0 + \epsilon u_1 + \epsilon^2 u_2 + O(\epsilon^3) \quad (5)$$

where u_0 is the background wave, u_1 is the first order scattered wave and u_k is scattering for higher orders.

$$u_1(r,\omega) = \omega^2 \int g_0(r,x,\omega)\, V(x) u_0(x,\omega)\, dx. \quad (6)$$

This is the first order Born approximation at receiver point r. As we go far from point source s to receiver r, the first order approximation is expressed in terms of Green's function is written as:

$$u_1(r,s,\omega) = \omega^2 s(\omega) \int g_0(r,x,s,\omega)\, V(x)\, dx. \quad (7)$$

In ray theory background, Green's function is towards the high-frequency approximation, which is expressed in terms of travel time $T(x,y)$ and amplitude $A(x,y)$ at location x for point source y is mathematically written as:

$$g_0(x,y,\omega) = A(x,y)\exp[i\omega T(x,y)] + O(\omega^{-1}). \quad (8)$$

By inserting equation (8) in equation (7), we get:

$$u_1(r,s,\omega) = \omega^2 s(\omega) \int A(r,x,s)\, V(x) \exp[i\omega T(r,x,s)]\, dx. \quad (9)$$

This is known as the general equation for wave scattering by frequency domain Born approximation in an acoustic medium.

3. Methodology

First of all, velocity-depth models are simulated with the help of MATLAB coding for further analysis. Velocity variations in different models are assumed to suit various lithological formations normally encountered in sedimentary formations. For the modelling purpose, the travel time is calculated through that velocity-depth model by the principle of the ray-tracing method. At that point, the reflectivity series of the corresponding model is figured; which is in terms of the ratio between reflected and incident wave fields. Later, the Common Shot Gather (CSG) data is generated aid with reflectivity series and followed by imaged boundary required for Kirchhoff's prestack migration. The modelling process undergoes without smoothing the velocity models. To play out the whole process, we design an end-on survey with Ricker wavelet as the mother/source wavelet. The entire clarified strategy is accomplished with a better shot sampling rate at every alternate shot point.

3.1 *Computational procedure*

A new code with the help of MATLAB environment is developed to generate various velocity-depth models. Accordingly, the essential code for the reflectivity series generation and travel time calculation of the respective velocity models is improved from the existing MATLAB code provided by Utah Tomography and Modelling/Migration Consortium (http://utam.gg.utah.edu). All the examples were computed with the help of a computational system configured with an 8-node quad-core i7 processor CPU @ 3.10 GHz with 16 GB RAM. All the parameters used to develop the model and the parameters extracted from the data are mentioned in table 1. All the above processing steps are executed with the help of the MATLAB technical computing language. Kirchhoff's migration gives better results when the lateral gradient of the linear velocity function (Kz) is 0.6, but to test whether our proposed approach is capable or not to handle the high-velocity variation, we consider the lateral gradient as 0.8 for our study (20% more than the normal value).

4. Numerical results

To make sure the efficiency of the proposed technique, six different geological models (both structural and stratigraphic) are assumed by assigning an appropriate model dimension. These models are mostly assembled by a number of complicated interfaces. All those interfaces are composed of points in the distance–depth domain. These models are created by means of formation of P-wave velocity. Velocity variation is well-thought-out in vertical as well as horizontal direction of all assumed models. The technique is applied over both the structural as well as stratigraphic traps because the seismic signatures over the stratigraphic models are typically more complex as compared to structural models. We designed an end-on spread type survey by keeping the source in left at the beginning for all proposed models and processed with 38 Hz central frequency of the Ricker wavelet. To avoid aliasing effect in

Table 1. *List of relevant parameters used for modelling.*

Model name	No. of time samples (nt)	Spatial sampling interval (m)		Travel time space (MB)	Execution time (sec)
		Calculated	Assumed		
Salt dome	2091	13.15	10	5.6	9.91
Over thrust	1416	32.89	30	278.2	75.33
Unconformity	1415	10.52	10	38.1	24.09
Pinch-out	755	19.73	15	42.5	13.23
Reef	1076	20.77	20	5.61	7.39
Canadian over-thrust	2856	48.68	30	173.6	60.77

the data, spatial sampling interval plays an important role and that is calculated by the formula:

$$\Delta x \leq \Delta x_N = \frac{V_{\min}}{2f_{\max} \cdot \sin\theta} \tag{10}$$

where Δx is the spatial sampling interval, Δx_N is the spatial Nyquist sampling interval, $V_{\min}$ is the minimum velocity of the model, $f_{\max}$ is the maximum frequency and θ is the dip angle, which is considered as the maximum (90°) for the present analysis. Table 1 provides all parameters related to acquisition and processing.

4.1 *Salt dome*

The first example is a salt dome which is a type of structural trap formed when a hydrocarbon deposit found at the depth inside the surrounding strata. The velocity-depth model is shown in figure 1(a), designed using nx = nz = 100 grid points, where the velocity varies from 1000 to 3623 m/s at various depths. This model comprises six reflectors with a salt dome structure in the central position. The modelling process is performed with a spatial sampling interval of 10 m with total time sample nt = 2091 and time sampling interval dt = 0.005 s. Figure 1(b) represents the reflectivity model of the velocity-depth model. It is observed that the portion in between the reflectors of both the left and right-most side beneath the salt dome structure is not reflected.

The result of the forward modelling is illustrated in figure 1(c), which represents the CSG at current shot position no. 100. The CSG shows a number of hyperbolic events corresponding to various reflectors. From the migrated section illustrated in figure 1(d), it is observed that at the intermediate zone of the first and second layers, some smoothed region near about a depth of 500 m at the distance from 1400 m to the end is affected by some noises. At the position where there was no reflectivity series observed, it is unable to restore the amplitude frequently. The noise found in the migrated section might be because of the impact of overcritical reflection, which can be ignored. But from this, in general, the migrated section gives satisfactory results, from which one can interpret the actual complex image of the salt dome with its actual focal position.

4.2 *Over-thrust*

The second one is a well-known over-thrust model used by CREWES toolbox for various algorithm. The original model is of 501 × 1021 grid points. However, for the present analysis, it is resized into 625 × 625 grid points. The modification is done in order to prepare a reasonable model that can be processed so smoothly. The velocity-depth model shown in figure 2(a) is considered with a model dimension of 3.125 × 3.125 km that is suitable for acoustic medium. The minimum and maximum velocities of the model are 2500 and 4000 m/s, respectively. The modelling process is performed with a spatial sampling interval of 30 m with a time sampling interval of dt = 0.004 s. This model is comprised of many breakpoints focused at various depth levels. Figure 2(b) is the result of the reflectivity model of the corresponding velocity-depth model from which all the reflectivity series are recognized at its actual position. Like the previous model, the result after forward modelling is outlined in figure 2(c), which signifies as CSG at the current shot location no. 625 (extreme end shot point).

A number of hyperbolic events are seen along with direct and refracted waves all through the CSG data. The definite outcome of our concentration which is achieved after the migration is

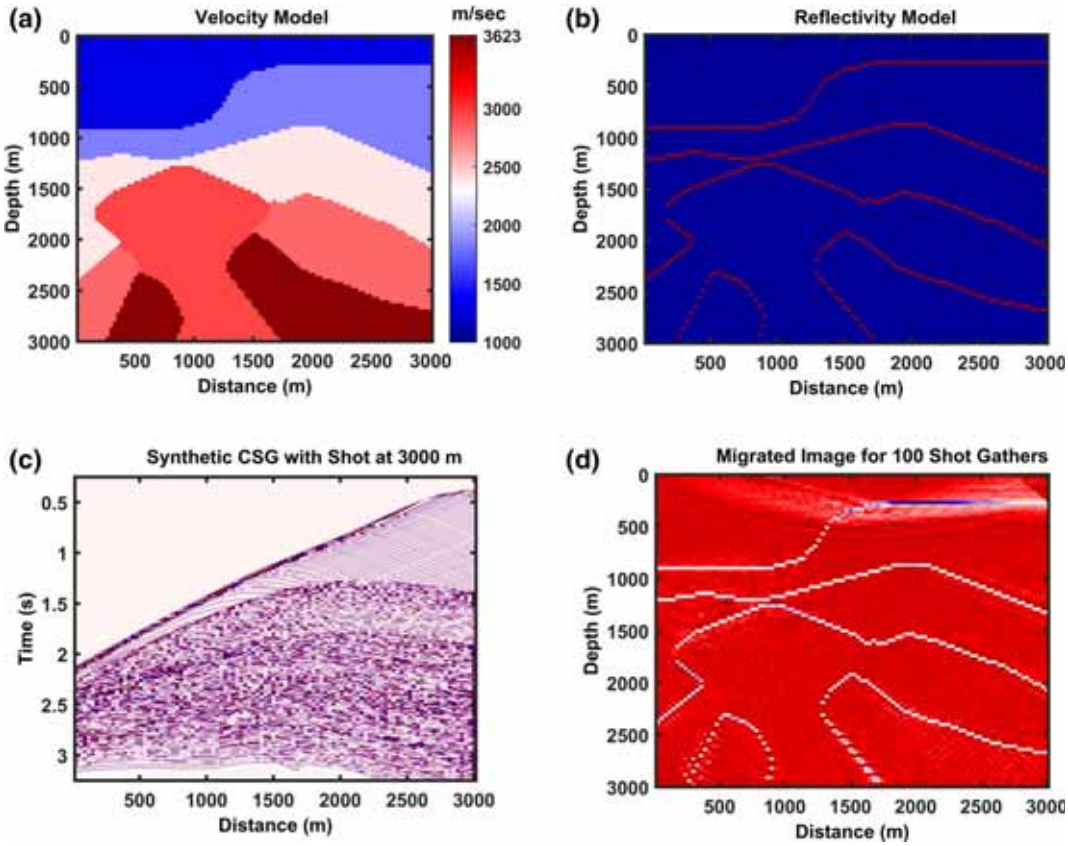

Figure 1. Schematic diagram of salt dome model. (**a**) Velocity-depth model, (**b**) reflectivity series of corresponding velocity-depth model, (**c**) common shot gather (CSG) data at current shot position, and (**d**) migrated image of the salt dome for total number of shot gathers.

illustrated in figure 2(d). It is observed in this migrated section that all the breakpoints of the thrust plane are noticeable in a reasonable way, restoring all the reflectors at their actual depth position. At the shallow depth, i.e., from zero to 200 m towards the right-end of the migrated section, a few noises are seen. This insignificant noise generated is nothing but the migrated noise of Kirchhoff's migration only. Except this, the amplitude restoration has occurred throughout the migrated section. All the breakpoints of the thrust are properly delineated at their true depth position. The migrated section also gives an attractive result in terms of imaging with no diffraction impact.

4.3 *Unconformity*

After successful implementation of the proposed technique over structural traps, to conclude the results a little bit more: the technique is further implemented over various stratigraphic traps.

The third example is an unconformity: which is a surface that separates two rock masses or strata of different ages indicating that sediment deposit is not continuous. Figure 3(a) represents the velocity-depth model for an angular unconformity. The model is designed by using a 200 × 200 grid points and dx = dz = 10 m. In this model, velocity varies from 800 to 2900 m/s with a high range difference both in vertical and in horizontal.

The forward modelling is performed with a spatial sampling interval of 10 m and time sampling interval of dt = 0.005 s. The model having one horizontal layer merged with the anticline structured layer and formed the unconformity layer. Beneath the unconformity layer, other reflectors are present, which featured an anticline structure with the help of dipping events.

It can also be seen that the velocity of the younger horizon one is low as compared to the older one. Figure 3(b) represents the characteristic of reflectivity series for the velocity-depth model. It is observed that all the reflectors can generate their corresponding reflectivity series at their actual depth position. The travel time to generate CSG data is recorded at this processing step. The CSG, which is obtained by applying forward modelling is

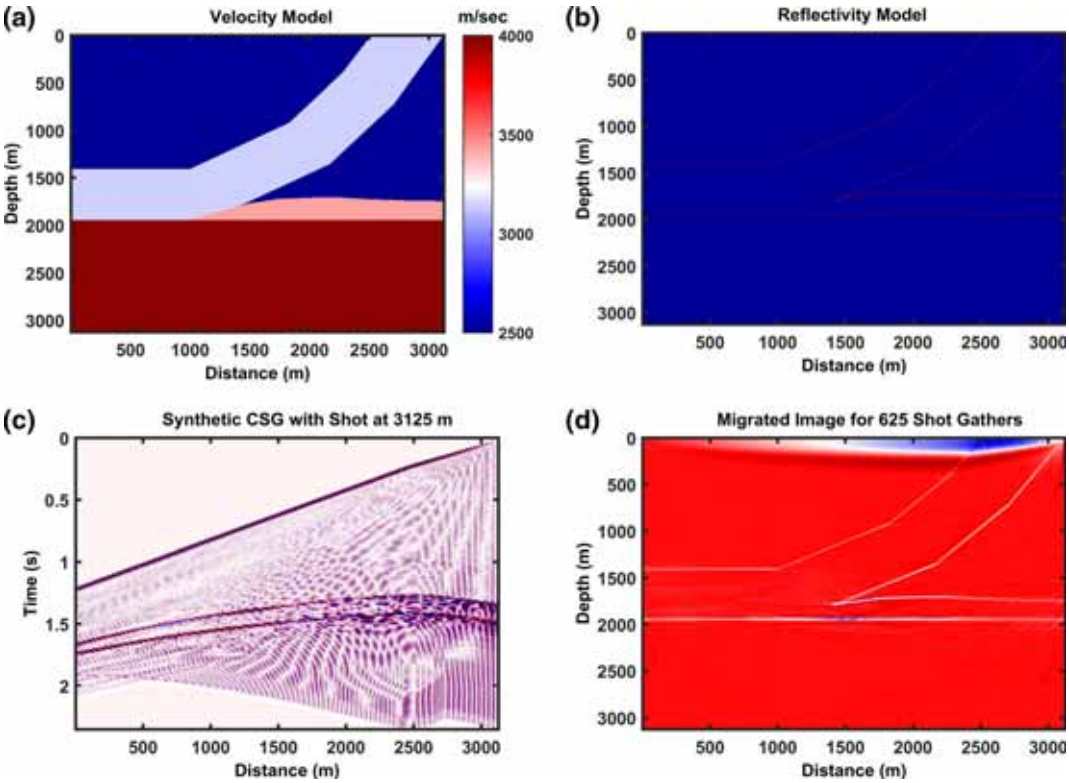

Figure 2. Schematic diagram of over-thrust model. (**a**) Velocity-depth model, (**b**) reflectivity series of corresponding velocity-depth model, (**c**) common shot gather (CSG) data at current shot position, and (**d**) migrated image of the over-thrust model for total number of shot gathers.

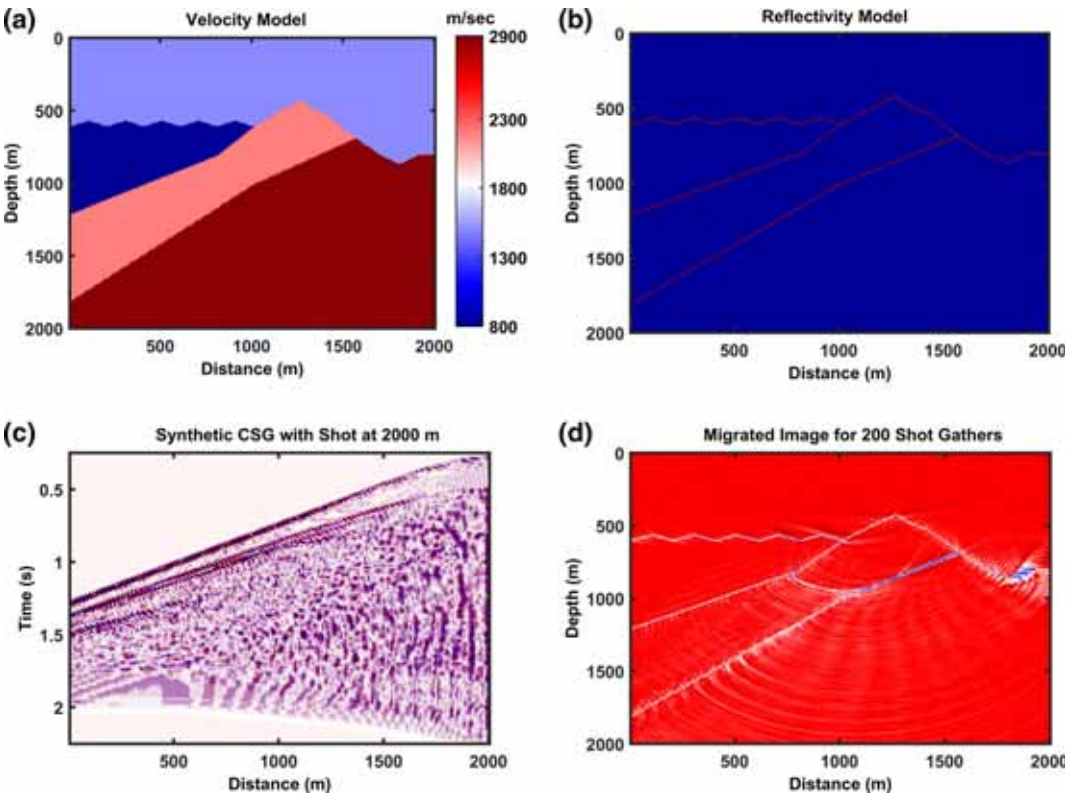

Figure 3. Schematic diagram of unconformity model. (**a**) Velocity-depth model, (**b**) reflectivity series of corresponding velocity-depth model, (**c**) common shot gather (CSG) data at current shot position, and (**d**) migrated image of the unconformity model for total number of shot gathers.

outlined in figure 3(c). A number of hyperbolic events are observed throughout the CSG. Figure 3(d) indicates the result of the migrated image after performing the Kirchhoff's migration. Here, it is seen that all the reflectors are repositioned to their actual depth position, but some amount of noise is generated at the extreme position of the younger strata. Diffractions are also found below the older strata, but the unconformity layer is clearly interpreted exactly as it is from the migrated section along with the anticline structure. The amplitude is restored properly throughout the result.

4.4 *Pinch-out*

The next example is pinch-out, which is a type of stratigraphic trap that a reservoir rock layer simply tapes off into a cap rock. It is normally seen in the extensional basins. Water in the reservoir rock will then force hydrocarbon into these traps from below. The velocity model for a pinch-out is represented by figure 4(a) where a pinch-out is taped off. The model is designed using grid points nx = nz = 200, where velocities are ranging from 1500 to 4000 m/s. The model consists of four inclined reflectors. The topmost reflector have a low inclination angle compared to other reflectors.

The second and third reflectors combine to complete the pinch-out feature which is divided into three segments. The dipper one having water forces the hydrocarbon into the traps which are accumulated at the upper part as oil and gas, is the actual subsurface configuration for any pinch-out feature.

Figure 4(b) represents the reflectivity series of the velocity-depth model. Here, it is noticed that all the reflectors have generated their corresponding reflectivity series at actual depth positions. By using forward modelling technique, CSG is generated. The processing is performed with a spatial sampling interval of 15 m and time sampling interval of dt = 0.005 s. After modelling, in CSG a number of hyperbolic events along with the direct arrivals are noticed which is illustrated in figure 4(c). Later, the Kirchhoff's depth migration method is applied over CSG. The result of the migration is shown in figure 4(d). From the depth migrated section, it is observed that all the reflectors are repositioned to their corresponding depth location.

The formation having saturated water, oil and gas zones within the pinch-out features also imaged clearly. But some noise is present at the shallow horizons which might be due to the numerical

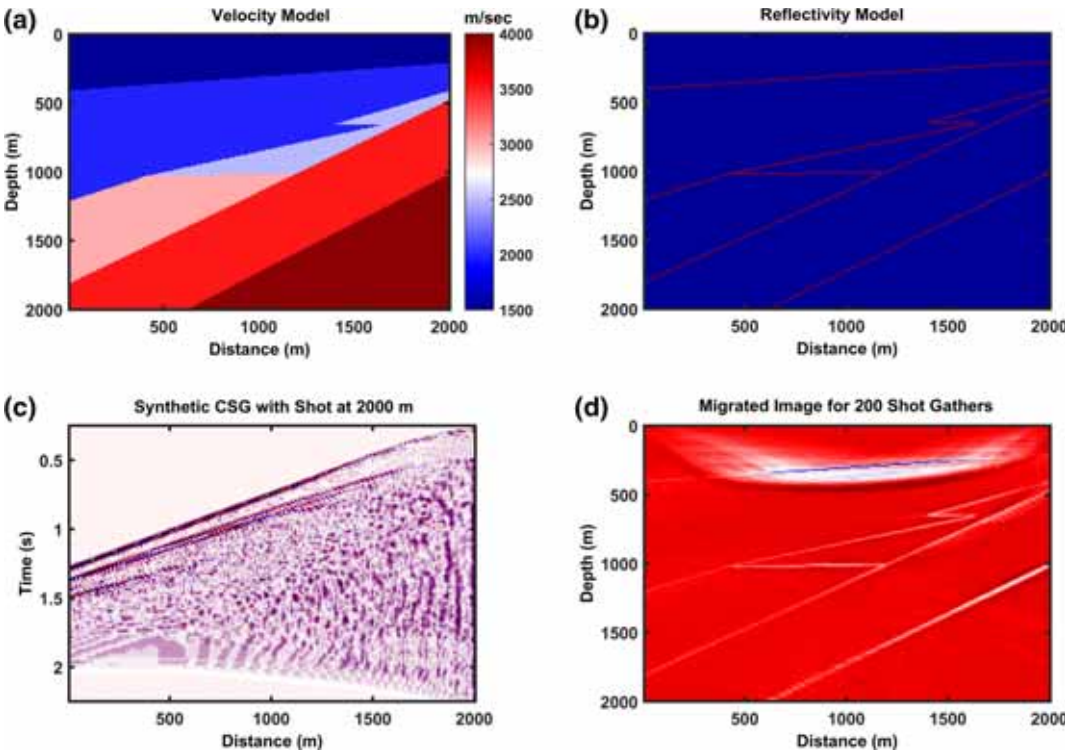

Figure 4. Schematic diagram of Pinch-out model. (**a**) Velocity-depth model, (**b**) reflectivity series of corresponding velocity-depth model, (**c**) common shot gather (CSG) data at current shot position, and (**d**) migrated image of the pinch-out model for total number of shot gathers.

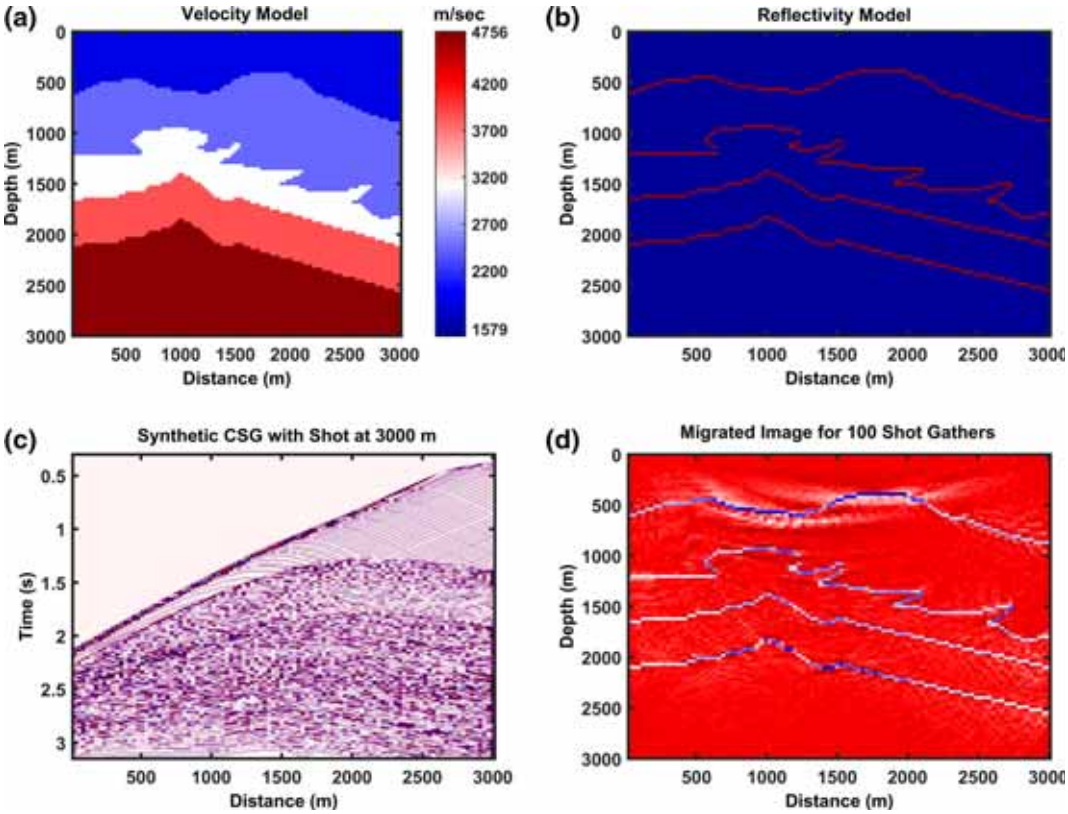

Figure 5. Schematic diagram of reef model. (**a**) Velocity-depth model, (**b**) reflectivity series of corresponding velocity-depth model, (**c**) common shot gather (CSG) data at current shot position, and (**d**) migrated image of the reef model for total number of shot gathers.

artefacts. In addition, the true amplitude also restored throughout the image.

4.5 *Reef*

All the above-defined models are generally encountered in the land seismic survey. The next example is a type of stratigraphic trap called as reef, always found in the marine environment.

A reef is a bar of rock or sand lying beneath the surface of the water. The reef structure within a sequence of sedimentary rocks provides a discontinuity which may serve as a trap or rise for the accumulation of hydrocarbon deposits.

Patch reef is one type of reef which usually occurs within the lagoon behind the barrier. To examine the proposed technique in this circumstance, a velocity-depth model is designed using nx = nz = 100. The velocities vary from 1579 to 4756 m/s at various depth levels, both horizontally and vertically. Figure 5(a) represents the velocity-depth model which consists of five dissimilar subsurface layers generated by four reflectors at 600, 1200, 1600 and 2100 m, individually. Along with this, the velocity-depth model consists of a total of four reef hubs at the beginning of the third layer of the subsurface.

From the reflectivity model represented in figure 5(b), it is noticed that each and every reflector are seen at its proper position as correlate with the velocity-depth model. The forward modelling process is performed with a time sampling interval of dt = 0.005 s whereas, the spatial sampling interval is 20 m. The result of this process termed as CSG is represented in figure 5(c), which shows some hyperbolic events, only for the current shot gather No. 100 at the distance of 3000 m. Figure 5(d) represents the migrated section for the total 100 shot gathers. The migrated depth section preserved all the reflectors at their actual depth position. Likewise, the amplitude preservation restored properly. As we specified beforehand, the ray tracing method is a high-frequency algorithm, some amount of noise appears in the middle of the shallow smoothed horizon at the depth of near about 600 m. This might be because of the impact of numerical artefacts; overall, the reef plane is properly sketched out all through the total profundity.

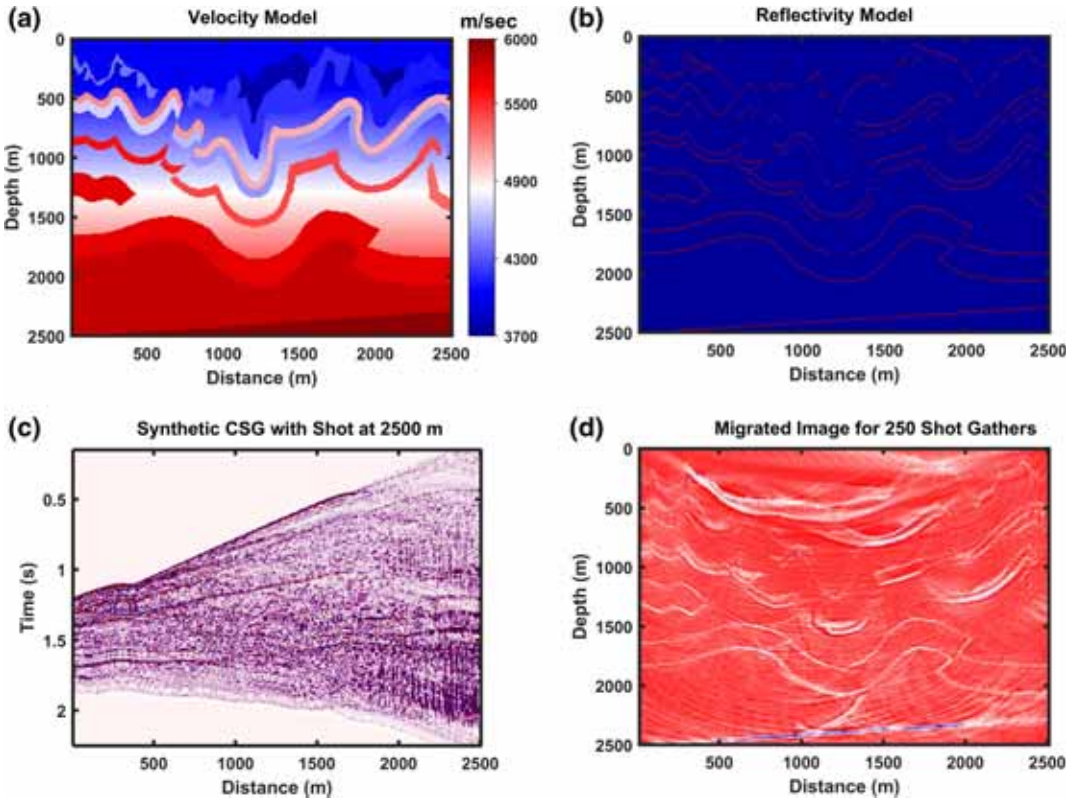

Figure 6. Schematic diagram of Canadian over-thrust model. (**a**) Velocity-depth model, (**b**) reflectivity series of corresponding velocity-depth model, (**c**) common shot gather (CSG) data at current shot position, and (**d**) migrated image of the Canadian over-thrust model for total number of shot gathers.

4.6 *Canadian over-thrust model*

Figure 6 represents the Canadian over-thrust model of Amoco and BP Oil Company. This model is considered, as it indicates more complex geological features. For our convenience to save the processing time, it is processed by using grid dimension of nx = nz = 250 points. The velocity varies from 3700 to 6000 m/s. The modelling is carried out with a spatial sampling interval of 30 m with a total shot of 250 where time sampling interval is dt = 0.006 s.

Figure 6(b) represents the reflectivity model of the velocity-depth model. Thus, in the reflectivity model, most of the reflectivity series are observed in the section with their true location. Figure 6(c) illustrated the modelling output in the form of CSG at the extreme end shot location No. 250. The final migrated result is shown in figure 6(d). The depth migrated section clearly delineated almost all the events by preserving its true amplitude. However, few reflectors at a depth of about 250 m did not appear in the final migrated section as it was not noticed in the reflectivity section. The overall structure has been clearly outlined having insignificant noise in the form of migrated noise.

5. Conclusions

In our proposed work, Kirchhoff's depth migration is performed with a modelling approach based on ART Born approximation. From the application, it is concluded that the seismic signatures over all the geological models brought out geological interfaces with their true depth location which has been seen in their corresponding reflectivity series. From all the reflectivity models, it is seen that the approximation was able to model partial reflections produced by continuous gradient, which is an advantage of this technique compared to others. As a result of forward modelling, in each CSG, it is observed that a number of hyperbolic events are generated corresponding to various reflectors at the current shot location of each reflectivity series. From the imaging point of view, the migrated section corresponding to all models delineates all the reflectors, restoring their characters properly. As we consider the lateral variation of velocity as

0.8, the complexity of the velocity-depth model does not create a big obstacle for both the modelling and imaging process and it also overcomes the problem related to velocity variation of the medium. The execution time to process a single shot in each model is mentioned in table 1. From this, it is also observed that the approach technique takes reasonable processing time and basically it depends on the number of time samples and travel time of each model. In case of the salt dome, it has been seen that when the dip angle is so high, at that particular region, reflectivity series did not produce properly. Some amount of noise is observed in the shallow horizon of most of the results. This is nothing but the migrated noise produced by Kirchhoff's. Except this, the numerical results maintained true amplitude for all the geological models. As a whole, the deeper events are imaged more clearly compared to shallow events. In general, because of the coherence and respective effectiveness with computational adequacy, the extended form of Born approximation technique along with Kirchhoff's depth migration is termed as a consequential technique towards seismic modelling and imaging.

Acknowledgements

The authors would like to thank the Department of Science and Technology (DST) Inspire Division, Govt. of India for the financial support through the Sanction No. DST/Inspire Fellowship/03/2014/IF140888. The authors also thank the reviewers and the editor for their constructive suggestions and comments, which improved the manuscript a lot.

References

Alaei B 2012 Seismic modelling of complex geological structures; In: *Seismic Waves-Research and Analysis: InTech* (ed.) M Kanao, Chap. 11, pp. 213–236.

Berkhout A J 2012 Combining full wavefield migration and full waveform inversion, a glance into the future of seismic imaging; *Geophysics* **77** S43–S50.

Capdeville Y, Larmat C, Vilotte J P and Montagner J P 2002 Numerical simulation of the scattering induced by a localized plume-like anomaly using a coupled spectral element and modal solution method; *Geophys. Res. Lett.* **29** 1318–1321.

Carcione J M, Herman G C and Ten Kroode APE 2002 Seismic modeling; *Geophysics* **67** 1304–1325.

Chapman C 2004 *Fundamental of Seismic Wave Propagation*; Cambridge University Press.

Chapman C H and Coates R T 1994 Generalized Born scattering in anisotropic media; *Wave Motion* **19** 309–341.

Clearbout J F 1985 *Fundamental of Geophysical Data Processing*; McGraw-Hill.

Dalton C A, Hjorleifsdottir V and Ekstrom G 2013 A comparison of approaches to the prediction of surface wave amplitude; *Geophys. J. Int.* **196** 386–404.

Huang X, Sun H and Sun J 2016 Born modelling for heterogeneous media using the Gaussian beam summation based Green's function; *J. Appl. Geophys.* **131** 191–201.

Jakobsen M 2012 T-matrix approach to seismic modelling in the acoustic approximation; *Stud. Geophys. Geod.* **56** 1–20.

Kirk P 1981 Vibroseis processing: *Developments in geophysical exploration methods*; Applied Science Publishers, London, **2** 37–52.

Panning M P, Capdeville Y and Romanowicz B 2009 Seismic waveform modelling in a 3-D Earth using the Born approximation: Potential shortcomings and a remedy; *Geophys. J. Int.* **177** 161–178.

Parisi L, Ferreira A M G and Capdeville Y 2015 Validity domain of the Born approximation for seismic waveform modelling in realistic 3-D Earth structure; *Geophys. J. Int.* **200** 910–916.

Peter D, Boschi L and Woodhouse J H 2009 Tomographic resolution of ray and finite-frequency methods: a membrane-wave investigation; *Geophys. J. Int.* **177** 624–638.

Romanowicz B A, Panning M P, Gung Y and Capdeville Y 2008 On the computation of long period seismograms in a 3D Earth using normal mode based approximations; *Geophys. J. Int.* **175** 520–536.

Tromp J, Tape C and Liu Q 2005 Seismic tomography, adjoint methods, time-reversal and banana-doughnut kernels; *Geophys. J. Int.* **160** 195–216.

Utah tomography and modelling/migration consortium, retrieved on 24.05.2016, from http://utam.gg.utah.edu.

Wang R, Jia X and Hu T 2004 The precise finite difference method for seismic modelling; *Appl. Geophys.* **1** 69–74.

Corresponding editor: N V Chalapathi Rao